arXiv:0804.1833v1 [cond-mat.mes-hall] 11 Apr 2008

Device Model for Graphene Nanoribbon Phototransistor

Victor Ryzhii[1,4], Vladimir Mitin[1,2], Maxim Ryzhii[1,4], Nadezhda Ryabova[1,4], and Taiichi Otsuji[3,4]
[1] *Computational Nanoelectronics Laboratory, University of Aizu, Aizu-Wakamatsu, 965-8580, Japan*
[2] *Department of Electrical Engineering, University at Buffalo, Buffalo, NY 14260-1920, USA*
[3] *Research Institute for Electrical Communication, Tohoku University, Sendai, 980-8577, Japan*
[4] *Japan Science and Technology Agency, CREST, Tokyo 107-0075, Japan*
(Dated: April 11, 2008)

An analytical device model for a graphene nanoribbon phototransistor (GNR-PT) is presented. GNR-PT is based on an array of graphene nanoribbons with the side source and drain contacts, which is sandwiched between the highly conducting substrate and the top gate. Using the developed model, we derive the explicit analytical relationships for the source-drain current as a function of the intensity and frequency of the incident radiation and find the detector responsivity. It is shown that GNR-PTs can be rather effective photodetectors in infrared and terahertz ranges of spectrum.

Photodetectors for far infrared (FIR) and terahertz (THz) ranges of spectrum are conventionally made of narrow-gap semiconductors and quantum-well structures. In the former case, interband transitions due to the absorption of photons are used. The operation of the detectors based on quantum-well structures is associated with the electron or hole intraband (intersubband) transitions [1, 2]. Some time ago, quantum-dot and quantum-wire detectors were proposed [3, 4]. The transition from quantum well structures with two-dimensional electron (hole) spectrum to low-dimensional structures such as quantum-wire and quantum-dot structures might lead to a significant improvement of the FIR and THz detectors (see, for instance, ref. [5] and the references therein). The utilization of *graphene*, i.e., a monolayer of carbon atoms forming a dense honeycomb two-dimensional crystal structure [6, 7, 8, 9, 10] opens up tempting prospects in creation of novel FIR and THz devices [11, 12, 13, 14, 15], in particular, novel photodetectors. One of the most promising metamaterials for FIR and THz detectors is a patterned graphene which constitutes an array of graphene nanoribbons (GNRs). The energy gap between the valence and conduction bands in GNRs as well as the intraband subbands can be engineered varying the shape of GNRs, in particular, their width, which can be defined by lithography. [16, 17, 18]. This opens up the prospects of creation of multicolor photodetectors.

In this paper, we propose of a graphene nanoribbon phototransistor (GNR-PT) and evaluate its performance using the developed device model. The detector proposed has a structure of GNR field-effect transistor consisting of an array of GNRs with the side source and drain contacts (to each GNR) sandwiched between the highly conducting substrate and the top gate electrode. The operation of devices with similar structure were explored recently (see, for instance, [17, 18, 19, 20, 21, 22, 23]). Here, we study The structure of GNR-PT under consideration is schematically shown in Fig. 1. For the sake of definiteness, we consider a GNR-PT with optical input from the bottom of the structure assuming that the substrate and the layer sandwiching the GNR array are transparent.

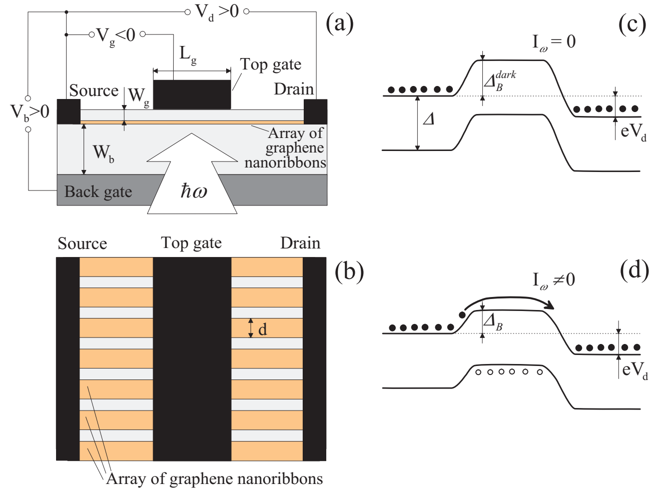

FIG. 1: Schematic view of GNR-PT structure side (a) and top (b) views, as well as the device band diagrams under dark condition (c) and under irradiation (d). Circles in panels (c) and (d) corresponds to electrons and holes.

Graphene nanoribbons exhibit the energy spectrum with a gap between the valence and conduction bands depending on the nanoribbon width d:

$$\varepsilon_n^{\mp}(p) = \pm v\,\sqrt{p^2 + (\pi\hbar/d)^2 n^2}. \tag{1}$$

Here $v \simeq 10^8$ cm/s is the characteristic velocity of the electron (upper sign) and hole (lower sign) spectra, p is the momentum along the nanoribbon, $\hbar$ is the reduced Planck constant, and $n = 1, 2, 3, ...$ is the subband index. The quantization corresponding to Eq. (1) of the electron and hole energy spectra in nanoribbons due to the electron and hole confinement in one of the lateral directions results in the appearance of the band gap $\Delta = 2\pi\hbar/d$ between the valence and conduction bands and in a specific the density of states (DOS) as a function of the energy.

The source-drain current along the GNRs associated with the electrons propagating from the source to the drain and overcoming the barrier in the center section of the channel (beneath the top gate), can be presented in the following form:

$$J = e\Sigma_b v_T \exp\left(-\frac{\Delta_B}{k_BT}\right)\left[1 - \exp\left(-\frac{eV_d}{k_BT}\right)\right]. \qquad (2)$$

Here, $\Sigma_b = (æ\, V_b/4\pi\, eW_b)$ is the electron density induced in the channel by the back gate voltage $v_T = v\sqrt{4k_BT/\pi\Delta}$ is the electron thermal velocity [23], $\Delta_B = -e\varphi_m$ is the height of the barrier in the central section of the channel, $\varphi_m < 0$ is the electric potential in its minimum. Equation (1) is valid if $V_d \ll V_b$ (but ratio eV_d/k_BT can be arbitrary). The quantities φ_m and Δ_B are determined by the gate voltages V_b and V_g and the electron and hole densities in the central section. The dependence of φ_m on the drain voltage V_d is weak provided that V_d is not too large and the length of the top gate layer $L_g \gg W_b, W_g$. The latter inequality imply that the "short-gate" effects are insignificant [22, 23]. Here W_b and W_g are the thicknesses of the layers separating the GNR array from the back and top gates, respectively.

In the absence of irradiation, eq. (2) leads to the following equation for the dark current: [23]

$$J^{dark} = v\left(\frac{æ\, V_b}{2\pi^{3/2}W_b}\right)\sqrt{\frac{k_BT}{\Delta}}$$

$$\times \exp\left(-\frac{\Delta_B^{dark}}{k_BT}\right)\left[1 - \exp\left(-\frac{eV_d}{k_BT}\right)\right], \qquad (3)$$

where $\Delta_B^{dark} = -e[W_bW_g/(W_b + W_g)](V_b/W_b + V_g/W_g)$ is the height of the barrier in the central section of the channel under the dark conditions with $V_b/W_b + V_g/W_g < 0$ in the operation regime, and æ is the dielectric constant.

Assuming that the photogenerated electrons are quickly swept out of the central section of the channel by the lateral (along nanoribbons) electric field, while the photogenerated holes are captured in this section, the hole density can be found considering the balance between their photogeneration and leakage into the source and drain regions.

The equation governing the balance of the photogenerated and thermal holes in the central depleted section of the channel, can be presented as

$$v_T\Sigma_g \exp\left(-\frac{\Delta_B}{k_BT}\right)\left[1 + \exp\left(-\frac{eV_d}{k_BT}\right)\right] = G_\omega L_g, \qquad (4)$$

where Σ_g is the density of holes photogenerated in the section of the channel beneath the top gate by the voltage applied to the latter, G_ω is the rate of photogeneration of holes, and L_g is the length of top gate, which is approximately equal to the length of the depleted section of the channel. The left-hand side of eq. (4) is the rate of the holes leaving the depleted region, whereas the right-hand side is the net rate of the hole photogeneration in this region. The effect of holes photogenerated in higly conducting source and drain sections of the channel is disregarded.

Considering eq. (4), and taking into account that in the gradual channel approximation [24] $\varphi_m \propto \Sigma_g$, we arrive at

$$\Delta_B - \Delta_B^{dark} \simeq -\frac{4\pi\, e^2W}{æ}\Sigma_g$$

$$\simeq -\frac{4\pi\, e^2L_gW}{æ\, v_T}\frac{\exp(\Delta_B^{dark}/k_BT)}{[1 + \exp(-eV_dk_BT)]}G_\omega, \qquad (5)$$

where $W = W_bW_g/(W_b + W_g)$. Equation (5) is valid if the electron density in the section of the channel under the top gate is small due to sufficiently strong depletion of this region by the negatively biased top gate and if the rate of photogeneration (i.e., the intensity of radiation) is moderate, so that $\Delta_B^{dark} - \Delta_B \ll \Delta_B^{dark}$.

Substituting Δ_B from eq. (5) into eq. (2) and considering eq. (3), we arrive at the following equation for the photocurrent $\Delta J = J - J^{dark}$:

$$\Delta J \simeq \left(\frac{e^2V_b}{k_BT}\right)\left[\frac{1 - \exp(-eV_d/k_BT)}{1 + \exp(-eV_d/k_BT)}\right]\left(\frac{W}{W_b}\right)L_gG_\omega. \qquad (6)$$

The rate of the photogeneration due to the interband absorption of incoming radiation is given by

$$G_\omega = \alpha_\omega I_\omega, \qquad \alpha_\omega = \left(\frac{4\pi}{c\hbar\omega}\right)Re\,\sigma_\omega^{inter}, \qquad (7)$$

where c is the speed of light, $\hbar\omega$ is the energy of incident photons, I_ω is the radiation intensity, and $Re\,\sigma_\omega^{inter}$ is the real part of the ac interband conductivity. Considering the energy spectrum of electrons and holes in nanoribbons, disregarding the degeneracy of the electron and hole gases and the polarization selectivity of the interband absorption, and following the procedure used previously [12], this quantity can be presented as

$$\mathrm{Re}\sigma^{inter}(\omega) = \left(\frac{e^2}{2\hbar}\right)\sum_{n=1}^{\infty}\frac{\Delta\cdot\Theta(\hbar\omega - \Delta_n)}{\sqrt{\hbar^2\omega^2 - \Delta_n^2}}. \qquad (8)$$

Here, $\Delta_n = \varepsilon_n^+(0) - \varepsilon_n^-(0) = n\,\Delta$, and $\Theta(\hbar\omega - \Delta_n)$ is the unity-step function. Considering eqs. (7) and (8), we obtain

$$G_\omega = \sum_{n=1}^{\infty}\frac{\beta\Delta\cdot\Theta(\hbar\omega - n\Delta)}{\sqrt{\hbar^2\omega^2 - n^2\Delta^2}}\frac{I_\omega}{\hbar\omega}, \qquad (9)$$

where $\beta = 2\pi\, e^2/c\hbar \simeq 2\pi/137 \simeq 4.59 \times 10^{-2}$. The quantity $\beta\Delta/\sqrt{\hbar^2\omega^2 - \Delta^2}$ is the effective quantum efficiency of the GNR array. In the limit $\hbar\omega$ tends to Δ, the quantum efficiency is limited by $\beta\Delta/\Gamma$, where Γ is the "smearing" of the valence and conduction band edges due to different imperfections.

Using eqs. (6) and (9), we obtain the following formula for the detector responsivity $R = \Delta J/L_gI_\omega$:

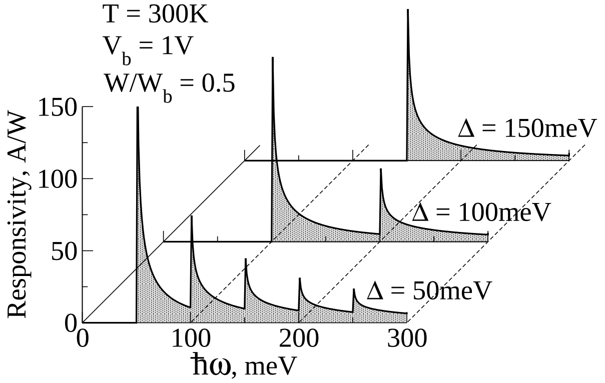

FIG. 2: Responsivity, R, as a function of energy of incident photons, $\hbar\omega$, for GNR-PTs with different band gaps, Δ.

$$R \simeq \left(\frac{W}{W_b}\right)\left(\frac{eV_b}{k_BT}\right)\left[\frac{1-\exp(-eV_d/k_BT)}{1+\exp(-eV_d/k_BT)}\right]$$

$$\times \sum_{n=1}^{\infty} \frac{e\beta\Delta\cdot\Theta(\hbar\omega-n\Delta)}{\hbar\omega\sqrt{\hbar^2\omega^2-n^2\Delta^2}}. \qquad (10)$$

It is instructive that the GNR-PT responsivity is independent of Δ_B^{dark}. This is because the effective lifetime of the photogenerated holes in the deleted section of the channel and, therefore, their density increases as $\exp(\Delta_B^{dark}/k_BT)$ (see eq. (4)). Using eq. (10) and setting $W \simeq W_b/2$ and $eV_d \gg k_BT$, the responsivity maximum (at $\hbar\omega \gtrsim \Delta$) and its ratio to the responsivity minimum (at $\hbar\omega \lesssim 2\Delta$) can be estimated, respectively, as follows:

$$\max R \simeq \frac{e\beta}{2\sqrt{2\Gamma\Delta}}\left(\frac{eV_b}{k_BT}\right) \propto \Delta^{-1/2}T^{-1}, \qquad (11)$$

$$\frac{\max R}{\min R} \simeq \sqrt{\frac{6\Delta}{\Gamma}}. \qquad (12)$$

Assuming that $\Delta = 100$ meV, $\Gamma = 2$ meV, $V_b = 1-5$ V, and $T = 300$ K, we obtain $\max R \sim 50-250$ A/W.

These values of the responsivity obtained significantly exceed those for intersubband quantum-well, -wire, and -dot photodetectors for the IR and THz ranges (see, for instance ref. 2). This is primarily due to higher quantum efficiency and higher photoelectric gain, which might be exhibited by GNR-PTs. The latter is associated with a long life-time of the photogenerated holes in the central section of the channel because these holes are confined in this section by relatively high barriers, so that the photoelectric gain $g \propto \exp(\Delta_B^{dark}/k_BT) \gg 1$. The maximum responsivity of GNR-PTs can also exceed the responsivity of the customary photodetectors made of narrow gap semiconductors (for example, PbSnTe and CdHgTe), whose responsivity is about a few A/W [1, 2], because the former can exhibit rather high quantum efficiency at the resonances $\hbar\omega = n\,\Delta$ arising due to the lateral quantization in GNRs.

As follows from eqs. (11) and (12), max R and min R markedly increase with decreasing T and Δ. Figure 2 shows the spectral dependences of the responsivity, R, of GNR-PTs with different energy gaps Δ (different width of GNRs) calculated using eq. (10). It is assumed that $W/W_b = 0.5$, $V_b = 1$ V, and $T = 300$ K.

The principle of the device operation limits the value Δ_B^{dark} and, consequently, the photoelectric gain g. The point is that when the height of the barrier under dark conditions Δ_B^{dark} is comparable with the band gap Δ, the density of thermal holes can be fairly high. As a result, these holes essentially affect the potential distribution in the channel that, in turn, weakens the dependence of Δ_B on the intensity of irradiation. Taking into account that the Fermi level in the case of devices with rather large electron densities in the source and drain sections of the channel is close to the bottom of the conduction band, the pertinent limitation can be presented in the following form: $\Delta - \Delta_B^{dark} = \Delta + eW(V_b/W_b + V_g/W_g) \gg k_BT$. In the above consideration we neglected the recombination of the phogenerated holes in the central section of the channel. The recombination of the photogenerated holes, primarily, due to the interband tunneling in the high-field regions between the quasi-neutral and depleted regions can, in principle, affect the photoelectric gain. This imposes a limitation on the increase of the responsivity R with decreasing energy gap Δ corresponding to eq. (11).

In conclusion, we developed the GNR-PT model and calculated the device characteristics. It was shown that GNR-PTs can surpass the IR and THz detectors utilizing other types of quantum structures (in particular, quantum-well, -wire, and -dot photodetectors). The GNR-PTs under consideration can exhibit substantial technological advantages, including easier integration with readout circuits, over the detectors on the base of narrow-gap semiconductors like PbSnTe and CdHgTe.

The work was supported by the Japan Science and Technology Agency, CREST, Japan. Partial support of the work at UB by the Air Force Office of Scientific Research, USA is also acknowledged.

---

[1] A. Rogalski: Infrared Phys. Technol. **38** (1997) 295.

[2] V. Ryzhii: ed. “*Intersubband Infrared Photodetectors*”,

World Scientific, Singapore, 2003.
[3] V. Ryzhii: Semicond. Sci. Technol. **11** (1996) 759.
[4] V. Ryzhii, et al.: J. Physique IV **6** (1996) C3-157.
[5] V. Ryzhii, et al.: Semicond. Sci. Technol. **19** (2004) 8.
[6] C. Berger, et al.: J. Phys. Chem. **108** (2004) 19912.
[7] K. S. Novoselov, et al.: Nature **438** (2005) 197.
[8] A. K. Geim and K. S. Novoselov: Nat. Mater. **6** (2007) 183.
[9] J. Hass, et al: Appl. Phys. Lett. **89** (200) 143106.
[10] T. Ando: Physica E **40** (2007) 213.
[11] V. Ryzhii: Jpn J. Appl. Phys. **35** (2006) L923.
[12] L. A. Falkovsky and A. A. Varlamov: Europ. Phys. J. **56** (2007) 281.
[13] O. Vafek: Phys. Rev. Lett. **97** (2006) 266406.
[14] V. Ryzhii, A. Satou, and T. Otsuji: J. Appl. Phys. **101** (2007) 024509 1-5.
[15] V. Ryzhii, M. Ryzhii, and T. Otsuji: J. Appl. Phys. **101** (2007) 083114 1-4.
[16] K. Nakata, et al.: Phys. Rev. B **54** (1996) 17954.
[17] B. Obradovich, et al.: Appl. Phys. Lett. **88** (2006) 142102.
[18] Z.‘Chen, et al.: Physica E **40** (2007) 228.
[19] B. Huard, et al.: Phys. Rev. Lett. **98** (2007) 236803.
[20] G. Liang, et al.: IEEE Trans. Electron Devices, **54** (2007) 677.
[21] G. Fiori and G. Iannaccone: IEEE Electron Device Lett. **28** (2007) 760.
[22] V. Ryzhii, M. Ryzhii, and. T. Otsuji: Appl. Phys. Express **1** (2008) 013001
[23] V. Ryzhii, et al.: arXiv:cond-mat/0801.1543.
[24] M. Shur, *Physics of Semiconductor Devices* (Prentice Hall, New Jersey, 1990).